International Journal of Chemical, Materials and Biomolecular Sciences
ISSN: 2415-6620
Vol:15, No:7, 2021

# Introduction to Electron Spectroscopy for Surfaces Characterization

Abdelkader Benzian

***Abstract*****—**Spectroscopy is the study of the spectrum produced by the radiation-matter interaction which requires the study of electromagnetic radiation (or electrons) emitted, absorbed, or scattered by matter. Thus, the spectral analysis is using spectrometers which enables us to obtain curves that express the distribution of the energy emitted (spectrum). Analysis of emission spectra can therefore constitute several methods depending on the range of radiation energy. The most common methods used are Auger electron spectroscopy (AES) and Electron Energy Losses Spectroscopy (EELS), which allow the determination of the atomic structure on the surface. This paper focalized essentially on the Electron Energy Loss Spectroscopy.

***Keywords*****—**Dielectric, plasmon, mean free path, spectroscopy of electron energy losses.

## I. Introduction

THERMODYNAMICALLY, the statistical interpretation of the physical phenomena depends on the possibility of treating them as a gas model in which a solid can be adequately represented by a mixture of electron and phonon gases. To some extent it was not easy to develop the atomic model of matter proposed by Greek philosophers, especially Democritus, to a molecular model of gas, looking for gas properties like a susceptibility to expand in free space (represented by the volume and the temperature), exerting pressure on the walls of a container. From the corpuscular standpoint, electromagnetic radiation has properties similar to a gas, from its propagation in free space, as well as it exerts pressure on a wall (surface) in its path. Based on this analogy, light is treated as an ensemble of photons that move freely and straight, and collide with a surface, so that they can penetrate and reflects [3]. Light is characterized by frequency $\nu$ and according to *Lambert's first law* (the passage of light through matter); Light is able to penetrate any surface and is absorbed in it so that it penetrates deeper into the material where the frequency $\nu$ becomes progressively less intense, according to:

$$I(x) = I(0)e^{-\epsilon x} \tag{1}$$

where $\epsilon(\nu)$ is the extinction coefficient, which depends essentially on the frequency of the penetrating light. In order to develop this model, an atom can be thought of as a target bombarded by particles of light, thus, they are absorbed by the atom as a result of this bombardment, which leads to the excitation of the atom from a state 1 to a higher energy state 2 where the energy of the absorbed photon has been used. Given the probability of a direct hit in a certain ratio, that is, the atom must have an effective cross-section $\sigma_{12}$ defining this ratio or possibility, thus, the number $N$of unexcited atoms can be calculated from their initial number $N(0)$ according to the law ($n$ is the density of photon gas) [3]

$$N = N(0)\exp(-x\, n\sigma_{12}) \tag{2}$$

while the atom returns to the ground state by losing a quantum of energy estimates as $h\nu = E_2 - E_1$. This process corresponds with Einstein's prediction for the generation of luminous flux from a medium of excited atoms [3]. One can say that this excitation is collective vibration of the atoms of bulk as well as of surface when occurs an exchange of quantum of energy between the atoms defined by a pulsation $\omega$ and called *plasmon* [13]; in addition, one can conclude that the generating of another quasiparticle is the phonon looking for similarity with the sound waves. Collective vibration expressed by the plasma oscillation is interpreted by the creation of plasmon, each plasmon carries a quantum of energy defined by its frequency $\omega_p$, and energy $E_p = \frac{h}{2\pi}\omega_p$ (see Section V in this paper) which refers to bulk plasmon energy. If this energy is considerable this refers to inelastic scattering. Another phenomenon that can happen is the interband transition; the electron is able to transfer to higher shell out of its particular shell (electronic level or orbital), and this requires a quantity of energy equivalent to the binding energy of the electron corresponding to its particular shell. Using the law of conservation of energy, the binding energy of an electron can be calculated from [15]:

$$h\nu = E_{kin} + e\varphi + E_b \tag{3}$$

where $h\nu$ is the quantum energy of primary radiation, $\varphi$ is the work function of an electron, and $E_{kin}$ and $E_b$ are the kinetic and *binding energies* of an electron, respectively. So, the $\varphi$ is the energy enough to remove an electron from the metal, in which the frequency $\nu$ must be greater than the frequency $\nu_0$ if we set that $\varphi = h\nu_0$ Fig. 1, where $E_F$, the maximum energy (Fermi level) of the electrons of the conduction band of the solid at a temperature of 0 $K$. As an example: the electronic configuration of Lithium atom is $1s^2 2s^1$, photoemission of an electron from level 1 leads to get $Li^+$ ion according to the interaction, $Li + h\nu \rightarrow Li^+ + e$. Then the kinetic energy $E_{kin}$ of the photoelectron is given by

$$E_{kin} = h\nu + E(\mathrm{Li}) - E(\mathrm{Li}^+) \tag{4}$$

Aek. Benzian is with the Laboratoire de physique des particules et physique statistique, Ecole Normale Supérieure Kouba-Alger, Algérie (e-mail: benzian8@gmail.com).

where there are two possibilities for electronic configuration $Li^+$ $[1s^1 2s^2]$, one can observe *two photoelectron peaks* due to this photoemission.

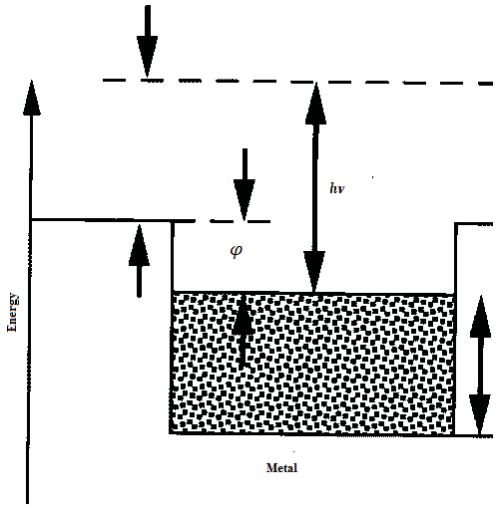


Fig. 1 The electron emitted from solid surfaces

Note that the wave function that is obtained as a solution of the Schrödinger equation given by [11]

$$\psi_0(x) = \left(\frac{m\omega}{\pi\hbar}\right)^{1/4} exp\left(-\frac{m\omega}{2\hbar}x^2\right) \quad (5)$$

and it represents the ground state of an oscillating particle that its probability of the presence in its ground state is given by

$$|\psi_0(x)|^2 = \left(\frac{m\omega}{\pi\hbar}\right)^{1/2} exp\left(-\frac{m\omega}{\hbar}x^2\right) \quad (6)$$

where its curve appears as a Gaussian curve, the probability of its maximum presence is located at position x = 0 (position of equilibrium). Then we can deduce that these excitations produce electron-hole pair, this pair forms a quasiparticle known by Exciton, for two electric charges $+q$ at position $r$ and $-q$ at position $r'$, the energy potential is given depends on the dielectric constant $\varepsilon$ as

$$V(r - r') = q\phi(r - r') = -\frac{q^2}{\varepsilon|r-r'|} \quad (7)$$

$(\phi(r - r') \; is \; the \; potential)$.

As the volume and the surface become polarized, the excitation then gives a meaning of energy loss when the primary beam of photons penetrates the incident surface of the solid and scattered inside, it loses a quantity of energy before its backscattering from the surface to the vacuum. Now and as said before, the excitation does not involve the volume only but also the surface, the displacement of charges along the boundary of the surface produces an electric field with two components, one parallel component $(E_x)$ and another $(E_z)$ perpendicular to the boundary, magnetic field, therefore, has one component $H_y$ [1], [12]. When the longitudinal waves of the surface charge density $\rho(r)$ circulate along the surface as a polarization wave and expressed by Maxwell' equation as $\nabla E = {}^{\rho}/_{\varepsilon_0}$ ($\varepsilon_0$ is the vacuum primitivity which equals to one), therefore, the charge density at the boundary is written as [4], [1]:

$$\rho(r|_{z=0}) = \rho(x,t) = \frac{1}{4\pi}[E_z\,(z = 0^-) - E_z(z = 0^+)] \quad (8)$$

The electric field follows the relation $E(z) = \nabla\phi(z)$, as well as the potential describing the plasmon written by

$$\phi(x,t,z) = \sin(qx - \omega t)\exp(-q|z|) \quad (9)$$

which is a solution of Laplace's equation, when the volume density of the electric charge is null [2], $q$ and $\omega$ are the wavevectors and angular frequency of oscillation and $t$ represents time. And for continuity of the electric field, we consider Fig. 2 that illustrates the boundary of the solid by a semi-infinite substrate with complex dielectric constant $\varepsilon_b$ and a surface layer of thickness $d$ with dielectric constant $\varepsilon_s$ (Fig. 2) [12].

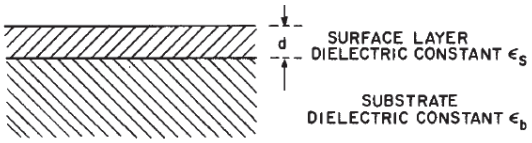


Fig. 2 The semi-infinite substrate with complex dielectric constant $\varepsilon_b$ and a surface layer of thickness d with dielectric constant $\varepsilon_s$

One can define the surface by $d \rightarrow 0$. The charges displace parallel to the wave vector $q_x$ which lies in the boundary, (Fig. 3) displays the situation of a p polarized surface wave.

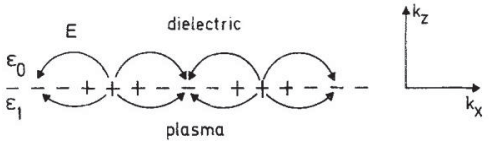


Fig. 3 Field configuration of a p polarized surface plasmon on a plasmon boundary

As the electric field of the incident electron is a cause of the generation of the plasmon, the electromagnetic wave can produce a similar effect, this allows us to conclude that the spectrum of energy loss has a relation with the dielectric properties from the surface. Then [13]

$$Im\left[\frac{-1}{\varepsilon(\omega)}\right] = \frac{\varepsilon_2}{\varepsilon_1^2 + \varepsilon_2^2} \quad (10)$$

is considered as an energy loss function, where $\varepsilon\,(\omega)$ is a complex permittivity whose real and imaginary parts are $\varepsilon_1$and $\varepsilon_2$ (Fig. 4). Therefore, the example of InSb (Fig. 5) showed a number of peaks represented by the loss function $Im\left[\frac{-1}{\varepsilon(\omega)}\right]$ and located between the frequencies 10 ev and 40 ev, the

peaks with frequencies less than 6/10 ev are due to different interband transitions where they occur from deeper levels (at small energies). Moreover, Fig. 5 shows a dominated volume plasmon peak that observing near 12,7 $eV$ (this value is shown in table 5.1 in [14])

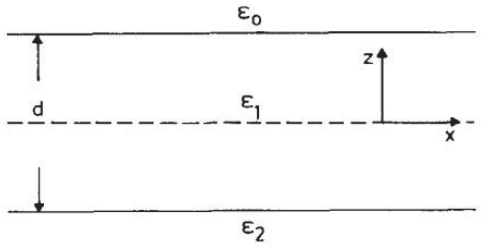


Fig. 4 Complex permittivity, ($\varepsilon_1$) real and ($\varepsilon_2$) imaginary parts, $\varepsilon_0$ (vacuum permittivity)

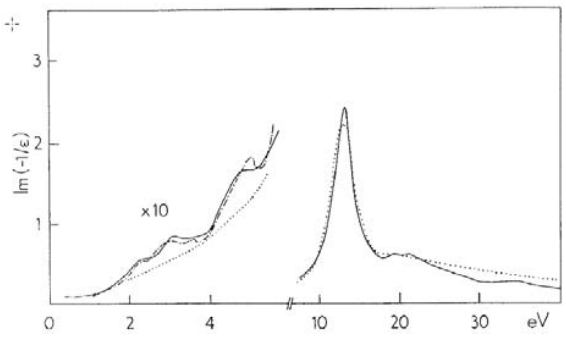


Fig. 5 The energy loss function of InSb, Full line: single crystalline, dash-dotted: polycrystalline, dotted line: amorphous InSb [14]

## II. Electron Scattering

The advance in the study of the surface state of materials needs to develop methods for surface analysis that employs the Electron Spectroscopy that interests by spectrum analysis. To identify essentially the chemical elements in the materials surfaces and their concentration, and therefore their geometrical arrangement, we rely on the characterization methods that are non-destructive methods and very high sensitivity towards surfaces and interfaces namely Auger electron spectroscopy (AES), Energy Loss Spectroscopy (EELS) as well as the Elastic Peak Electron Spectroscopy (EPES). The surface state of these materials is the most important matter in that the surface structure and reactive properties help classify the materials according to the required functions. Different methods of surface analysis can meet these conditions, but their ability is often different. The information obtained from each of them may not be sufficient, and thus combining them allows us to examine and determine the properties of materials more efficiently. There are two important matters in this field: first matter relates by a physical quantity known as *the mean free path*, the kinetic energy of incident electrons that bombard the solid surface must take a value in a certain range that allows the electron to reach enough distance (without losing a significant amount of energy, for the measurement of this distance be more exact [17]) which includes the first surface layers, this distance is known as the mean free path. Therefore, primary electrons beam with kinetic energies in the range 50-1000 ev that fall on the surface has a very short mean free path (less than 10 A°) [14]. Then, under the thermodynamical conditions, since the electrons of the valence band considered as a perfect gas as mentioned before, the expression of mean free path λ is given by Avogadro's number $N_A$, the temperature $T$, and the pressure $P$. Thus, the molecules can be treated as a hard-sphere with a diameter $d$ of each molecule; one can consider the molecule in motion that moves a distance $D$ before colliding with another molecule as well as the quantity $\sigma = \pi d^2$ is the collision cross section (effective area of a target molecule). Thus, it may to employed the law of the perfect gas when D represents *the mean free path* $\lambda$ to formulate the law that gives $\lambda$ in termes of the mumber of the molecules $n$ per volume, where $n = \frac{N_A P}{RT}$ [18, Ch.2]

$$\lambda = \frac{RT}{\sqrt{2}\pi d^2 N_A P} \tag{11}$$

When the electrons travel into the material they decay exponentially according to *the Beer-Lambert relationship* given by

$$I(x) = I_0 \exp\left(-\frac{x}{\lambda}\right) \tag{12}$$

due to the inelastic scattering, where λ is the attenuation length of the electrons (less than the IMFP by 10% mostly [8]). $I_0, I$ are the primary current and the current of the reflected electrons, respectively. Spectroscopy provides information thanks to the depth that the primary beams of electrons reached which given by the mean distance $x$ with $x > d$ (or $|x| < |d|$) [3].

*The second matter* is the binding energy that appears as energy function that allows to determine the nature of the chemical species present at the surface. By definition the binding energy is the ionization energy required to completely remove an electron from its particular shell. Then the excitation of the valence band by photon or electron bombardment gives specific elemental information of surface thanks to measurements of the kinetic energy of electrons ejected from a solid after that. As we can see, the binding energy holds an atomic identity [1].

## III. Elastic and Inelastic Backscattered Electrons

Electrostatic forces are exchange forces between constituents of the atoms make the incident electrons that penetrate the solid interact with these constituents. Then if these incident electrons cause excitation of the electrons of the surface we say that it is an inelastic scattering of the primary electrons that are correlated by energy loss. If there is no energy loss or it is negligible, we say that this situation is expressed as elastic scattering, (the negligible energy loss reflects the meaning of very small excitation), and the primary electrons, typically, scattered with a small angle in the average

of (10 _ 100 mrad) for primary energy of 100 kev. This interaction which is characterized by an energy loss in which the elementary electrons lose part of their energy before they reflect from the surface causes what so-called an excitation of plasma to appear as an exchange of energy between the atoms of surface layers as discussed next. [5]. Fig. 6 shows: (a) backscattered electron (b) inelastic scattering of an electron with loss of energy by the inner shell (c) inelastic scattering of an electron with loss of energy by the outer shell) [5]. We demonstrate the mechanism for the elastic collision to occur by assuming a thicker sample of thickness d, where the signal travels from the B layer (substrate) to the A surface layer of material; here the signal suffers attenuation before it is emitted from the surface. And this attenuation is related to depth (Fig. 7) [8]. Therefore, the intensity of the emitted electron at an angle $\theta$ to the surface normal from the depth (mean distance $x$) greater than $d$ is,

$$I = I_0 \exp(-x/\lambda_{A,B} \cos\theta) \quad (13)$$

where $I_0$ is the incident intensity of transmission electrons on the surface (on the uniform substrate), $\lambda$ is the attenuation length for electrons emitted from layer B. This configuration expressed the elasticity of scattering by remarking the lack of linearity in the results illustrated in Fig. 7 [8], [3].

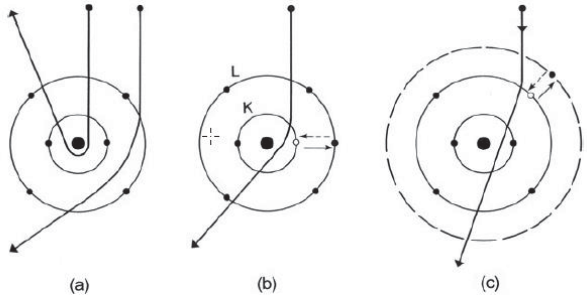


Fig. 6 The different electron-atom collision processes

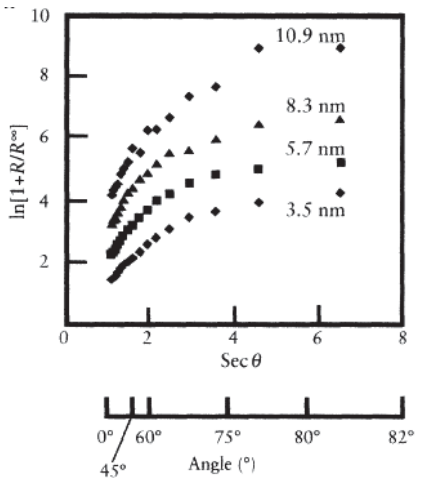


Fig. 7 The attenuation length for electrons elastic scattering

Note that the ratio of these signals [8] is $R = I_A/I_B$, $R^\infty = I_A^\infty/I_B^\infty$, rearranging and taking the natural logarithm

$$\ln[1 + R/R^\infty] = d/(\lambda_A \cos\theta) \quad (14)$$

Some of the incident electrons, generally 0.1 to 1%, are scattered from the surface without appreciable loss of energy, it is the basis of Elastic Peak Electron Spectroscopy which **is** associated with the detected electrons which have the same energy as the incident electrons (due to the negligibility of transfer energy) [7]. The characteristic of elastic scattering is that the energy transferred by the incident electron to the target is negligible, where this negligibility is mainly due to the fact that the electron mass to the nucleus mass is very insignificant. For an electron of kinetic energy $E_0$, rest mass $m_0$ deflected elastically through an angle $\theta$ the electron must transfer to the nucleus (mass $M$) an amount of energy $E$ given by [13]:

$$E = E_{max} \sin^2\left(\frac{\theta}{2}\right)$$

where $E_{max}$ is the maximum possible energy transferred that corresponding to $\theta = \pi$ rad.

$$E_{max} = 2E_0(E_0 + 2m_0c^2)/Mc^2 \quad (15)$$

The mean energy of the elastic peak $E$ is determined by $Ep = E_0$ of the primary electrons. The exact position of the elastic peak maximum $E = E_0 - E_{max}$. Because the rest mass of the electron is negligible relative to the nucleus mass i.e., $M \gg m$, (15) reduces to (see (4.3) in [7]):

$$E_{max} = \left(\frac{4m_0}{M}\right) E_0 \quad (16)$$

Furthermore, the spectrum of some emissions shows a small peak that characterized the electrons that have kinetic energy not depending on the incident electron energy. These emissions are known as Auger electrons. Often, they are corresponding with emissions related to the incident energy of the electrons, which is caused by the excited atom returning to stability through the loss of a quantity of energy in the form of X-rays. Auger electrons are produced as a consequence of the XPS process often referred to it as X- AES.

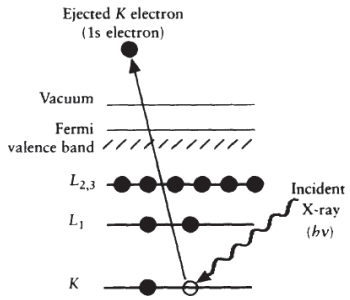


Fig. 8 Auger emission caused by X-ray

The relationship between the physics quantities in XPS is $E_B = h\nu - E_K - W$, where, $h\nu$ is the photon energy, $E_K$ is the kinetic energy of the electron and $W$ is the work function (Fig. 8) [8]. Once an atom has been excited in some way it is seeking to return to its ground state as the principle of energy conservation. Furthermore, it is possible that the core hole (consider K shell) that an electron ejected from it is filled by an electron from higher-level as the $L_{2,3}$ level for example (or another like$M_{2,3}$....), where another electron must be ejected from the atom; this electron which termed as KLL is the Auger electron (Fig. 9) [8], [1].

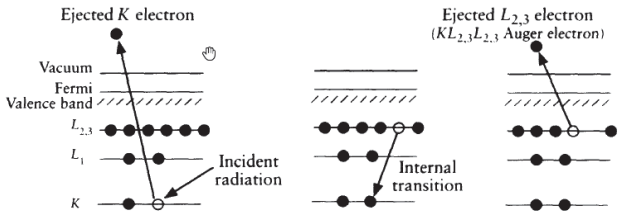


Fig. 9 Auger transition correlates with Ager emission

The Auger energy electron due to Auger transition shown in Fig. 9 is given by

$$E_{KL_1L_{23}} = E_k - E_{L_1} - E_{L_{23}} \quad (17)$$

The probability for an electron traveling a distance of $x$ in the solid without any elastic collision is $\exp(-x/\lambda)$, thus, 95% of the Auger signal that emerges at 90° come within $3\lambda$ of the surface. The sampling depth of $3\lambda$ can be reduced to $3\lambda\cos\theta$ from the sample surface normal for electrons emerge at a certain angle $\theta$ (Fig. 10) [6].

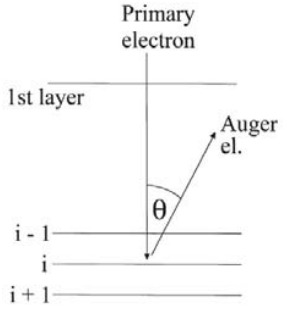


Fig. 10 Auger emission corresponds to the scattering angle

Fig. 11 showed the differential spectrum and direct energy of the Auger emission where $N(E)$ denotes the number of backscattered electrons for energy $E$. The differential spectrum is often recorded rather than the direct energy spectrum, because the spectrum of the latter contains not only Auger electrons but all the other emitted electrons.

The peak of the transition LMM is represented by two coordinates, the ordinate N which is the largest number of ejected electrons, and the abscissa E which is their energy at about 930 eV (referred by the dashed line). According to what appears from Fig. 11, Auger spectroscopy uses to gain information on the surface composition. Fig. 12 shows the different processes (emissions) that occur when an incident beam penetrates a surface of a solid. One can say that the Scattering of an electron beam inside a thin sample can be produced: The dotted area referred to the X-ray emission, the hatched area referred to the emission of the energy loss, Auger electrons are ejected from a small depth of 3λ.

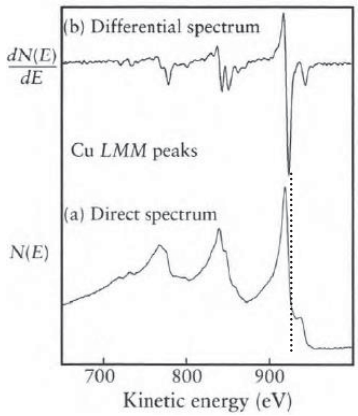


Fig. 11 Auger spectrum for Cu-LMM, (a) direct spectrum, (b) differential spectrum [8]

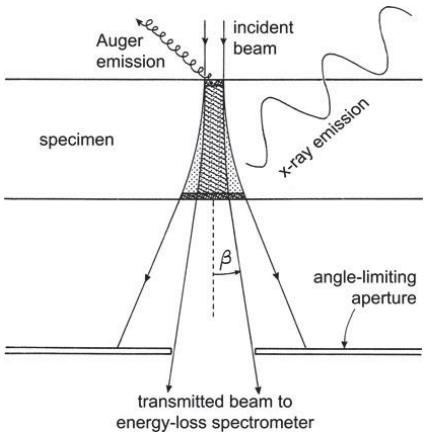


Fig. 12 Scattering of an electron beam inside a thin sample

## IV. Electronic Band Structure

### A. Zeeman Effect

Dutch physicist Pieter Zeeman (in 1896) has realized experimentally the first observation to a phenomenon of the splitting of the atomic energy levels when the atom is affected by a uniform external magnetic field $B$, this phenomenon becomes called the Zeeman effect [9] (Fig. 13). In fact, the generic nature of the anomalous Zeeman effect (with weak magnetic fields) states that the splitting of spectral lines cannot be explained in terms of orbital angular momentum only which leads to deduce the spin angular momentum s (or simply, the spin) that explains the splitting of the original spectral line into sub-lines and s here takes integers as well as half-integer values. It was introduced in quantum mechanics

as an attempt to explain the experimentally observed fine structures of the spectral lines in the emission spectra. The energy level $E$ splits up into $2l+1$ ($l$ takes the values $l = n-1$, where $n$ is any energy level of the atom) discrete energy levels, the $(2l+1)$ coinciding sub-levels with respect to each other in such a way that the distance between any two discrete sub-levels equals $\hbar\omega_l$ where $E(energy\ level) = E'(sublevel) - \hbar\omega_l m_l$. $m_l$ is the magnetic quantum number takes (2$l$ +1) values from $-l\ to\ l$ and $\omega_{l_{(Larmor\ frequency)}} = \frac{eB}{2m_e}$.

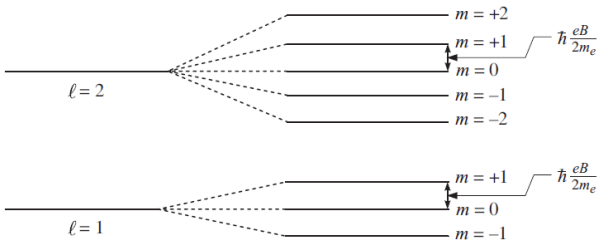


Fig. 13 Zeeman effect in the presence of an external magnetic field

*B. Interband Transitions*

Plasma oscillations in for a given value of the wave vector $q = q_c$ marked severe damping and this indicates that it is possible for the plasmon to transfer all its energy to a single electron, which can then dissipate the energy by passing over to higher levels of energy. This process is known as *the interband transition, the absorbed energy makes the electron transfer to another higher energy band of crystal*. Collective oscillations decay when plasma oscillations take a value that exceeds a theoretical value $q_c$ to exciting an electron ($q_i$) of the Fermi sea ($q_F$) to a higher energy level and so creating a hole. This limit, say that it breaks the resonance defined by bulk plasmon frequency $\omega_p$. Then it defines the critical wave vector $q_c$ at the maximum value of $q_i$ which equals $q_F$; $q_F$ is the Fermi wavevector that corresponds to Fermi velocity given as $v_F = {\omega_p}/{q}$. It can express the possibility of energy transfer by the closeness of the phase velocity to Fermi velocity. [14], [5]. As the results of [5] and because of the relativistic effects to the electrons that contain due to its electromagnetics interactions, the orbital momentum $L$ and the spin $S$ are not conserved separately; only the total angular momentum $J = L + S$ is conserved. For this reason, the exact energy levels must be characterized by the values $J$ of the total angular momentum. By given values $l\ and\ s$, the total moment $J$ is characterized by values noted $j$ [10], [11]:

$$j = l + s, \qquad l + s - 1, \ldots\ldots\ldots |l - s|$$

So, each value of $l$ defines a level of energy X, thus $l = 0$, 1, 2, 3, 4… correspond X: s, p, d, f, g, … respectively. Based on the values of the total moment $J$ which are the characteristic values of energy levels, we denote to each level by the notation $^{n}\mathbf{X_j}$. For example, the symbols $^2P_{1/2}$, $^2P_{3/2}$ denote levels with $l = 1, s = \frac{1}{2}, j = \frac{1}{2} and j = \frac{3}{2}$. The gas spectrum can be produced in an arc bursting inside a gas chamber. For hydrogen, we obtain a spectrum of lines located in the infrared, the visible, and the ultraviolet, depending on the experimental conditions. According to these results, Balmer [11] formulated the law that gives the wavelength $\lambda = \frac{c}{\nu}$ of nine spectral lines located in the visible spectrum, by:

$$\frac{1}{\nu} = -\frac{1}{hc}(E_n - E_m) \tag{18}$$

where $h$ is Plank's constant. During this emission of energy, the atom passed from a state where its energy was $E_m$ to an $E_n$ state where $E_n$ - $E_m$ = $h\nu$. As we say before, the orbital momentum $L$ and the spin $S$ are not conserved separately only the total angular momentum $J = L + S$ is conserved. The relative correction of first-order energy levels is given by:

$$E_{nj} = -\frac{m_e\alpha^4c^2}{2n^3}\left[\frac{1}{j+\frac{1}{2}} - \frac{3}{4n}\right] \tag{19}$$

We will *demonstrate subsequently* that the passage from one level of fine structure to another is only possible according to certain selection rules which limit the possible transitions. Let $\Delta x = x' - x$ denote the difference between two quantum numbers, with $x;\ x' = l, j\ ou\ m_j$. The only permitted values are: $\Delta l = \pm 1, \Delta j = 0, \pm 1, \Delta m_j = 0, \pm 1$. These possible values constitute the selection rules. Thus, for example, the transition between the states of structure fine $^3d_{5/2}$ and $^2P_{1/2}$ does not exist because it corresponds to $\Delta j = 2$. One says that it is a prohibited transition. The spectrum of emission lines represented by X-rays of a level $A$ immediately above to a level $B$ holds an identity of the atom. Typically, it is a hole in the $K$-shell for example which is filled by an electron from the $L$ -shell, this transition is denoted $K_\alpha$, another example, the transition from layer $M$ to layer $L$ is called $L_\alpha$ (Fig. 14).

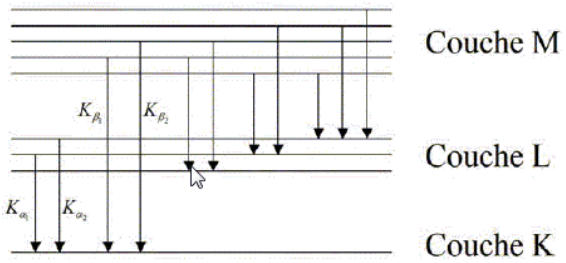


Fig. 14 Different spectral lines in the atomic couches represented by X-rays [19]

In addition, we note here that the vertical transitions between the band states which are distinguished by zero momentum transfer $\Delta q_{\|} = 0$ are a special state of semiconductors with direct-gap [2] (Fig. 15) (BZ indicates zone boundary on the graph).

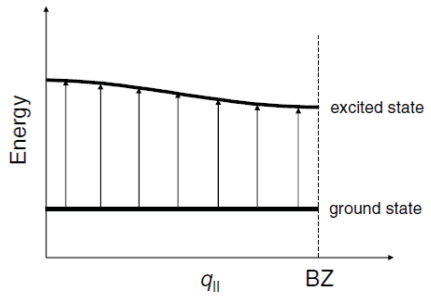


Fig. 15 The transitions from the ground state and the first excited state

## V. Electron Energy-Loss Spectroscopy

### A. Introduction

Electron Energy-Loss Spectroscopy (EELS) allows realizing a quantitative and qualitative analysis of the outermost atomic layers of surface; the analysis of the energy spectrum of low-energy electrons backscattered from the solid holds necessary information to identify the status of the surface. [12] An electron beam carries a primary energy $E_1$ incident on the solid and causes excitation of electrons of surface and interfaces (at most two or three). This excitation is vibrational modes near the surface when it is translated by a collective effect with energy $\hbar\omega_0$ that takes the form of a longitudinal traveling wave and thus backscattered into the vacuum with energy $E_2 = E_1 - \hbar\omega_0$. Then, the collective effect is known as a plasma resonance [5], [12] ($\hbar\omega_0$ *is the energy transferred to the plasma denoted by* $E_{max}$).

When an incident electron is absorbed, it loses a part of its energy to an electron from a lower level that is occupied, which with a certain probability allows this electron to be excited to the upper level. And this showed up in the scattered electron energy distribution as a peak at an energy $\Delta E$ below the elastic peak (Fig. 16), then say here that there is an energy loss respect to primary energy [6].

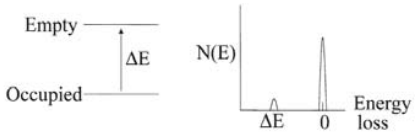


Fig. 16 Inelastic and elastic peaks comparison

The elastic peak at zero loss corresponds $E_{backscattered} = E_0$, and the magnitude of the energy loss $\Delta E$ is given by

$$\Delta E = E_0 - E_{backscattered} \tag{20}$$

which is equivalent to a quantum of energy expressed a vibrational mode that arises when the lost energy is absorbed by an electron of the solid, and thus expends it as vibration form [2], it is negligible in the elastic scattering and considerable in inelastic scattering.

The backscattered electrons thus carry information on only near the vicinity of the surface (see also section 4.5.1 in [15]).

The spectrum in Fig. 17 shows two-loss peaks at 59.5 meV and 256.5 meV for CO adsorbed from the surface of Ni.

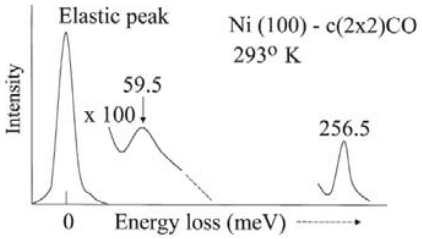


Fig. 17 Energy loss depends on the intensity of backscattered electrons

One can compare the intensity (peak magnitude) of spectra of energy loss (inelastic scattering) with the intensity of the spectra of elastic scattering to remark that the first is less than the second by the quantity ($\hbar\omega_0$) which is evidence for the vibrational mode of the electrons excitation [6] (see $E_{max}$ expression in this section).

### B. Energy Loss Function

As we said, the spectrum of energy loss has a relation with *the dielectric properties*, it can express the displacement $x$ of free-electron with mass $m$, by the equation of motion

$$m\ddot{x} + m\Gamma\dot{x} = -eE \tag{21}$$

And give the electric field $E$, that is the cause of generation of the plasmon, by (oscillatory field)

$$E(t) = E\exp(-i\omega t) \tag{22}$$

The equation of motion then has the solution:

$$x = \left({}^{eE}/_{m}\right)(\omega^2 + i\Gamma\omega)^{-1} \tag{23}$$

The parameter $\Gamma$ represents plasmon damping and is approximately the full width at half maximum (FWHM) of the plasmon peak in the energy-loss spectrum. Therefore, $\varepsilon(\omega)$ is a complex permittivity whose real and imaginary parts are $\varepsilon_1$ and $\varepsilon_2$. The displacement $x$ gives rise to a polarization

$$P = -enx = \varepsilon_0\chi E,$$

where $n$ is the number of electrons per unit volume and $\chi$ is the electronic susceptibility. The *relative permittivity* or *dielectric function* $\varepsilon(\omega)$ is then [5]:

$$\varepsilon(\omega) = \varepsilon_1 + i\varepsilon_2 = 1 + \chi = 1 - \frac{\omega_p^2}{\omega^2 + \Gamma^2} + \frac{i\,\Gamma\omega_p^2}{\omega(\omega^2 + \Gamma^2)} \tag{24}$$

Here $\omega$ is the angular frequency $(rad/s)$ of forced oscillation and $\omega_P$ is the natural or resonance frequency for plasma oscillation, given by

$$\omega_p = [ne^2/(\varepsilon_0 m)]^{\frac{1}{2}} \tag{25}$$

the term $Im\left[-\frac{1}{\varepsilon(\omega)}\right] = \frac{\varepsilon_2}{\varepsilon_1^2+\varepsilon_2^2}$, (10) is known as the *energy-loss function* at an energy loss $E = \hbar\omega$, thus

$$Im\left[-\frac{1}{\varepsilon(E)}\right] = \frac{E(\Delta E_p)E_p^2}{\left(E^2-E_p^2\right)^2+\left(E\Delta E_p\right)^2} \quad (26)$$

where $E_p$ is the plasmon energy and $\tau = {}^{1}/_{\Gamma}$ is a relaxation time. The energy-loss function $Im(-\frac{1}{\varepsilon})$ has a FWHM given by $\Delta E_p = \hbar\Gamma = {}^{\hbar}/_{\tau}$ [14] and reaches a maximum value of $\omega_p\tau$ at an energy loss given by

$$E_{max} = \left[E_p^2 - \left(\Delta E_p^2/2\right)\right]^{\frac{1}{2}} \quad (27)$$

So far, we know that a plasma oscillation of the loosely bound outer-shell electrons in a solid is equivalent to creating a *pseudo-particle* of energy $E_p = \hbar\omega_p$, known as a *plasmon.* Thus, we extract that there are longitudinal waves of charge density that travel along an external surface or an internal interface made up of a quantum that is surface plasmons, analogous to bulk plasmons. The component $E_z$ which is perpendicular to the surface decreases exponentially as [2, section 8.1]:

$$E_z = -q\phi_0 sng(z) sin(qx-\omega t) exp(-q|z|) \quad (28)$$

The perpendicular component of the electric field $E_z$ at the boundary is discontinuous when represented by [1] $E_z(z = 0^+) = \phi_0 q\, e^{i\,q\,x}$ and $E_z(z = 0^-) = -\phi_0 q\, e^{i\,q\,x}$ and the continuity of the electric field leads to the requirement,

$$\varepsilon_a(\omega) + \varepsilon_b(\omega) = 0 \quad (29)$$

where $\varepsilon_a$ *and* $\varepsilon_b$ are the relative permittivities on either side of the boundary (Fig. 2, where $\varepsilon_a = \varepsilon_s$). It must require $\varepsilon_b(\omega) = -1$ (see eq (7.33) of [2]). The simplest case is an interface between vacuum and a free-electron metal $\varepsilon_a(\omega) = 1$, and $\varepsilon_b(\omega) = 1 - \omega_p^2/\omega^2$, under the condition $\Gamma \longrightarrow 0$ [1]. So, it results that $\omega_p^2/\omega^2 = 2$, to find the solution of (29) as

$$\omega = \omega_p/\sqrt{2} \quad (30)$$

This solution represents the surface plasmon frequency $\omega = \omega_s = \omega_p/\sqrt{2}$ and gives $E_s = \hbar\omega_s$ the energy of the surface plasmon peak. From the relation between the electric field $E_z$ and the electric displacement field $D$, we write $\varepsilon(\omega)E_z(0^+) = \varepsilon' E_z(0^-)$ for a metal (with dielectric function $\varepsilon(\omega)$) in contact with a dielectric layer (with dielectric function $\varepsilon'$), rather than $\varepsilon_b(\omega) = -1$ (that related with the vacuum), we write

$$\varepsilon(\omega) = -\varepsilon' \quad (31)$$

Thus

$$\omega_s = \frac{\omega_p}{\sqrt{\varepsilon' + 1}} \quad (32)$$

The surface and volume contributions of energy loss are shown in Fig. 18, where the volume loss function takes its maximum value at the frequency 15 eV. By observation it, we can state the fact that surface-loss peaks occur at a lower energy loss than their volume counterparts, usually below 10 eV.

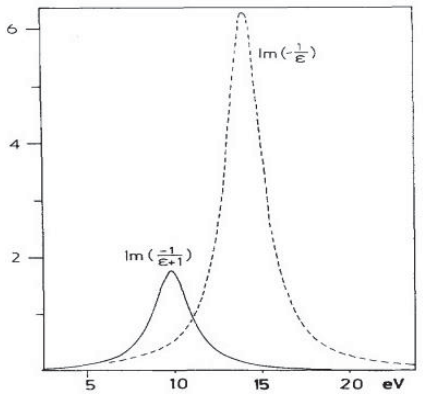


Fig. 18 Loss function for free electron gas: surface ≡ Im$(-\frac{i}{1+\varepsilon})$, volume ≡ Im$(-1/\varepsilon)$

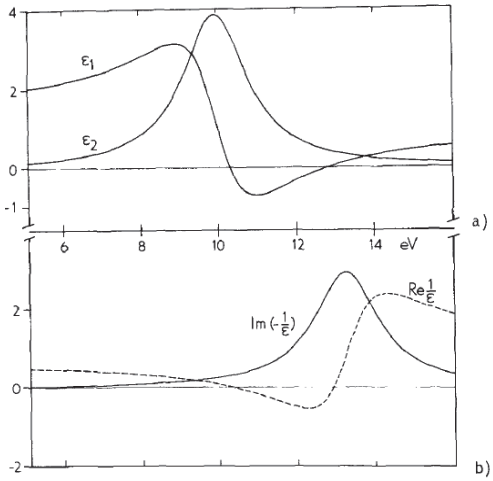


Fig. 19 The loss function of a bound electron: (a) The dielectric function: $\varepsilon_1$ real part, $\varepsilon_2$ imaginary part; (b) The function Im(-1/$\varepsilon$) (full line) and Re(1/$\varepsilon$) (dotted line) is calculated with $\varepsilon(\omega)$ of (a)

The interband transitions can be seen as peaks in the loss spectrum when the $\varepsilon_1$ is close to zero we observe a peak expresses the resonance frequency (Fig. 19) that shows the eigenfrequency corresponding to an interband transition at $\hbar\omega_n = 10\,eV$. After *the* $\varepsilon_1$ crosses the zero and displaces towards the positive values, the loss function Im(-1/$\varepsilon$) shows a peak with a maximum amplitude of $\varepsilon_2$ , therefore, from (10) we obtain (see Eq (1.11) in [14]):

$$Im\left[\frac{-1}{\varepsilon(\omega)}\right]_{max} = \frac{1}{\varepsilon_2(\omega_p)} = \omega_p\tau \quad (33)$$

Therefore, Fig. 19 shows the real part increasing and

decreasing the small imaginary part, this may indicate that longitudinal excitation exists as "a travelling polarisation wave" [5], [14]. On the other hand, the plasmon energy corresponds to the scattering vectors $q$, and energy $Ep(q)$ at which $\varepsilon_1$ passes through zero is determined by a longitudinal polarization wave defined by $div\ P \neq 0$ (P polarization, from where the displacement of electrons are forming a dipole momentum), and it is given by:

$$E_p(q) = E_p + \alpha(\hbar^2/m_0)q^2 \qquad (33)$$
$$\alpha = (3/5)E_F/E_p$$

where $E_F$ is the Fermi energy and (34) is a *dispersion relation* for the plasmon, $\alpha$ being the dispersion coefficient, Fig. 20 shows the increase in plasmon energy which is expressed by increasing of $q$.

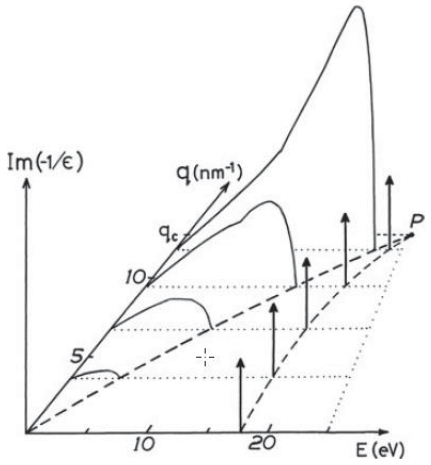


Fig. 20 The increase in plasmon energy of volume which expressed by increasing of $q$

Now we return to determining the mean free path by the quantities concerning the loss function mentioned for inelastic scattering. For an electron of creating a volume plasmon $\hbar\omega_p$ in a free-electron gas after having passed the thickness $D$ and being scattered inelastically into all angles up to $\theta_c$ (critical angle), the experiments show that these electrons, in general, have a multiples loss of $\hbar\omega_p$ not only one loss. Here we talk about an electron of creating a volume plasmon under the previous conditions with probability (given by relation (4.14) in [14]) $W$. By setting $W = 1$ and $D = \lambda$, with $v \sim c$ (relativistic region) the mean free path length $\lambda$ is given by [14]:

$$\boldsymbol{\lambda = \frac{\hbar v^2}{e^2\omega_p}\left(\ln\frac{vq_c}{\omega_p}\right)^{-1}} \qquad (35)$$

For a medium when $v < c$,

$$\lambda = \frac{2a_0E_0}{\Delta E}\left(\ln\frac{\theta_c}{\theta_{\Delta E}}\right)^{-1} \qquad (36)$$

where $\theta_E = \Delta E/(2E_0)$ is the characteristic inelastic scattering angle (see Eq (3.9) in [14]), $\Delta E$ is the energy loss or the energy of excited plasmon. For example, the numerical value of the mean free path in Al where $\theta_c \cong 13\ mrad$ for $E_0 = 50\ keV$ and $\Delta E = E_p = 15\ eV$ (Table 6.2 in [14]) is $\lambda = 800\ A°$.

*C. InP Surface Characterized by EELS and AES*

AES and electron loss spectroscopy (EELS) have been performed in order to study a (100) InP surface subjected to Argon-ion bombardment at low energy that results in the formation of a disordered layer [16]. Within the shape of In-MNN Auger electrons peak, about 114 of the total In atoms are of metallic type (the energies for plasmon excitation in (InP)dis and in pure metal In are similar, as discussed next) and they are associated with adsorbed phosphorus. Figs. 21 22 show the structure of In- $M_{45}N_{45}N_{45}$ Auger spectra and ELS spectra for: (a) after the introduction of the InP (100) sample in the spectrometer; (b), (c) and (d) effects of a 500 eV argon ion beam for increasing sputtering times: 15, 45 and 90 min; (e) after proton bombardment of the surface; (f) pure metallic In sample.

Fig. 21 shows an *attenuation* (see Section II) of the 15 eV loss peak, which emerges distinctly from the interlayers as revealed by the evolution of the spectra with primary electron beam energy $E$, and with the incidence angle (Fig. 22), this peak is characteristic of the crystalline InP (100) sample as volume plasmon of InP. The 8.6 eV and 11.5 eV values respectively (Fig. 21) correspond to the energies of the surface and volume plasmon of pure metal In. But this does not provide a certitude deduce that In islands had formed, the correlation between AES and ELS observations is more sufficient to conclude that. So, Fig. 23 expressed the evolution of the Auger ratio (P/B) during Ar-ion bombardment of the surface (100) InP, under incidence ion beam of 500 eV energy with a current density of $7.10^{-7}$ A.$cm^{-2}$. By definition: The P/ B value is the ratio of the height of the Auger peak between its maximum and the background linearly extrapolated from the high energy side, to the height of the background at the same energy. We calculate the ratio P/B to recognize the quantity of the content of each element on the surface since it depends on the height.

The measurements of the ratio of the Auger peak (P/B) are using a primary electron beam energy $Ep = 1850\ eV$ after a given time of argon ion bombardment of the surface. Interpreted the results of measurement are shown in Fig. 23 as the formation of disordered surface compound $(InP)_{dis}$, due to the damage caused by the argon-ion bombardment and including different chemical bonds represented by phosphorus and indium atoms (metallic In-In, covalent In-P, P-P...), one can see that if microdroplets are formed, they are certainly associated with adsorbed phosphorus. Fig. 23 also shows that the surface layer contains contamination was mainly composed of carbon (C- KLL) and oxygen (0- KLL) as revealed by AES.

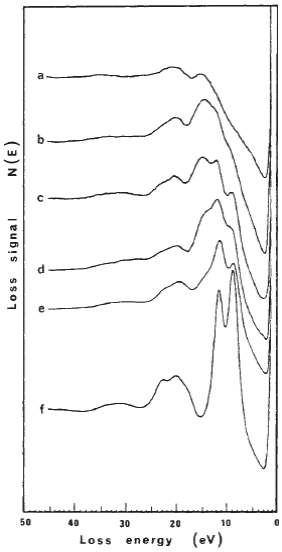


Fig. 21 Electron energy-loss spectra for a primary electron beam energy $E_p$ = 1000 eV, expressed the processes (a) (b) (c) (d) (e) and (f)

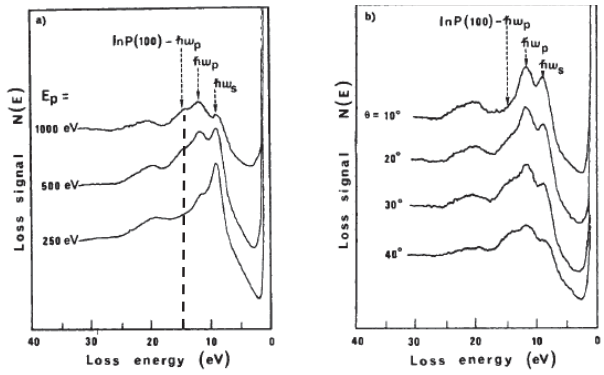


Fig. 22 Electron energy-loss spectra of the Ar+ etched InP (100) varied with: (a) the energy of the incident electrons; (b) the incidence angle $\theta$

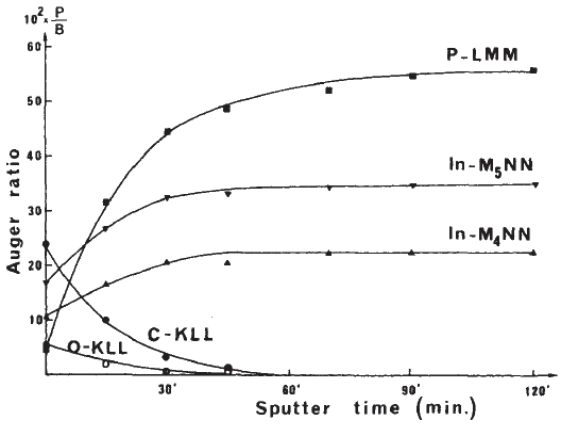


Fig. 23 The Auger ratio (P/B) Evolution during Ar-ion bombardment of the (100) InP surface, using a primary electron beam energy $E_p$ = 1850 eV

At 60 minutes, the P/B ratios reach constant values, where, the impurities become less than 0.01. It is the time of saturation when the pure metallic indium was formed. In addition, AES spectra shown in Fig. 24 are evidence that argon bombardment of the InP surface causes the formation of Indium metallic bonds and this is by comparing the loss energy of surface plasmon peaks at about 0,01 ev of pure In in (f) with (b), (c) and (d) when they seem similar (while this peak 0.01 ev does not appear clearly in (a)). Furthermore, we can distinguish the formation of metallic In from where the surface is damaged by argon-ion sputtering. Fig. 24 shows also an increase in metallic In contents (increase of N in the N(E) axis) depending on the time of the bombardment. The same observations of increasing in metallic In after proton bombardment of the surface (Fig. 24 (e)), but the In metallic content is great since proton bombardment makes more damage on the surface than the argon-ion. The comparison gives also the result that metallic In has remained in the covalent form (In bounded to P in InP) at 1,8 ev for the peaks of surface plasmon and 5 ev for the peaks of volume plasmon.

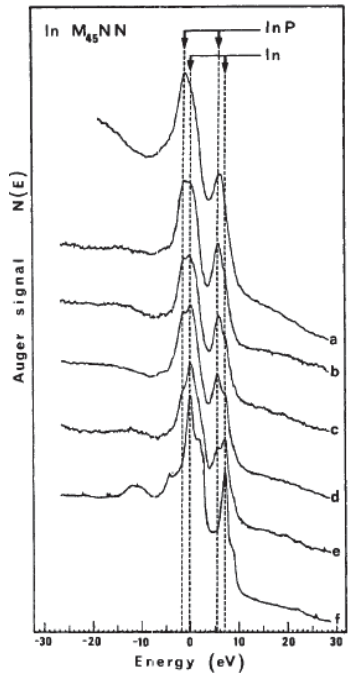


Fig. 24 Structure of In $M_{45}$ $N_{45}$ $N_{45}$ Auger spectra: (a) after the introduction of the InP (100) sample in the spectrometer; (b). (c) and (d) effects of a 500 eV argon ion beam for increasing sputtering times: 15, 45 and 90 min; (e) after proton bombardment of the surface;" the metallic In content is greatly enhanced; (f) pure metallic In sample

Surface reconstruction is realized by heat treatments of the sample and therefore restored the 15 eV loss peak which is the characteristic of the crystalline InP (100) sample. Thus, under the heat treatments, one can conclude that the AES and EELS spectra retain the same intensity in the different cases of the incident beam. This allows us to say that the heating allows a

better arrangement of the atoms and we do not notice any change in the different spectra. The improvement in the resolution of the energy loss signals is due to the fact that the surface does not present physical anomalies, and thus, the collection of backscattered electrons will be better. It is known that the presence of defects such as surface roughness leads to a decrease in the intensity of the elastic peak. Due to the high sensitivity of EELS and AES spectroscopies, we suggest that heating allows good reconstruction of the surface and InP by eliminating structural defects. This means that heating does not lead to desorption of the oxide and stabilizes the InP substrate by improving the homogeneity of the physical structure of matter [16].

## VI. Conclusion

The vibration mode of plasma allows to obtain the energy of surface plasmon and volume plasmon which are considered as the characteristic identity to the content of the chemical elements in the solid and which appear at the specters result from the collection of emitted rays by the surface. The work presented in this paper focuses on the characterization and study of the evolution of the physicochemical properties of the surfaces of materials subjected to different physical treatments, such as ion etching, electron irradiation, and heating. The electron spectroscopies AES, EELS, and EPES are non-destructive methods and very sensitive to surfaces and interfaces, when proved to be useful to determine the contamination layer on the InP surface that can be removed by surface cleaning with Ar ion bombarded. This process led to inducement the formation of the metallic indium islands and thus micro- droplets of phosphorus arise because of the damage of the bombardment. Moreover, the sensitivity of the electron spectroscopies that depend on the inelastic mean free path and incident energy emphasized that the heating treatment enables realizing the homogeneity of the surface.

## Acknowledgment

The Algerian Ministry of Higher Education and Scientific Research supports this research work. The authors are very grateful to the Algerian Direction Générale de la Recherche Scientifique et du Développement Technologique (DGRSDT) for the financial support.

## References

[1] Andrew Zangwil, Physics at Surface. Cambridge University Press (1988).
[2] Harald Ibach, Physics of Surfaces and Interfaces. Springer-Verlag Berlin Heidelberg 2006.
[3] A. I. Burshstein, Introduction to Thermodynamics and Kinetic Theory of Matter, Second Edition. 2005 Wiley-Vch Verlag Gmbh & Co. Kgaa, Weinheim
[4] Ansgar Liebsch, Electronic Excitations at Metal Surfaces, Physics of Solids and Liquids (1997).
[5] R.F. Egerton, Electron Energy-Loss Spectroscopy in the Electron Microscope, Third Edition. Springer Science+Business Media, llc 2011.
[6] Yip-Wah Chung, Practical Guide to Surface Science and Spectroscopy. Copyright _ 2001 by Academic Press.
[7] *G.* Gergely, elastic peak electron spectroscopy. Scanning vol. 8, 203-214 (1986) Facm, Inc.
[8] John F. Watts, John Wolstenholme, An Introduction to Surfaces Analysis by XPS and AES. Copyright © 2003 by John Wiley & Sons Ltd, The Atrium, Southern Gate, Chichester. West Sussex po19 8sq, England.
[9] Ajit Kumar, Fundamentals of Quantum Mechanics. Cambridge University Press (2018).
[10] E. Kogan, quantum Mechanics II. Researchgate (2019).
[11] Jean Hladik, Michel Chrysos, Pierre-Emmanuel Hladik, Lorenzo Ugo Ancarani, Mcanique Quantique - 3medition - Atomes et Noyaux. Applications Technologiques, Dunod Paris (2006).
[12] H. Ibach D. L. Mills, Electron Energy Loss Spectroscopy and Surface Vibrations. Academic Press, Inc (1982).
[13] R. F. Egerton, Electron Energy-Loss Spectroscopy in the TEM-r. Reports on Progress in Physics (2008).
[14] Heinz Raether, Excitation of Plasmons and Interband Transitions by Electrons. Springer-Verlag Berlin Heidelberg New York 1980.
[15] Anatoliy I. Kovalev and Dmitry l. Wainstein, Surface Analysis Techniques for Investigations of Modified Surfaces, Nanocomposites, Chemical, and Structure Transformations, (From Book Self-Organization during Friction (pp. 81 – 120)).
[16] C. Jardin and d. Robert, B. Achard, B. Grrizza and C. Pariset, An AES and ELS Study of InP (100) Surface Subjected to Argon Ion Bombardment. Surface and Interface Analysis, vol. 10, 301-305 *(1987).*